Maximising the physics potential of $B^{\pm} \to \pi^{\pm}\mu^{+}\mu^{-}$ decays

Alex Marshall[1], Michael McCann[2], Mitesh Patel[2], Konstantinos Petridis[1], Méril Reboud[3], Danny van Dyk[3]

October 26, 2023

Implications of LHCb measurements and future prospects - 2023

[1]University of Bristol, [2]Imperial College London, [3]Durham University,

Introduction

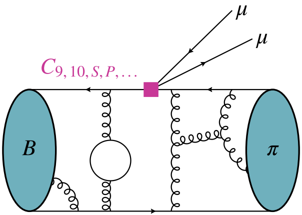

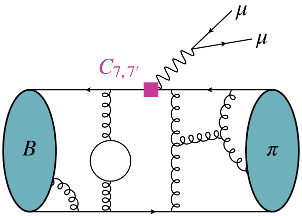

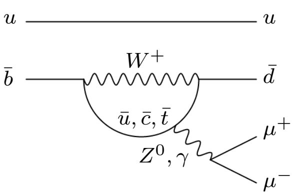

- Tensions exist with the SM in $B^\pm \to K^\pm \mu^+ \mu^-$.
- $B^\pm \to \pi^\pm \mu^+ \mu^-$ is highly suppressed in the SM, $|V_{ts}/V_{td}|^2 \approx 22$ times relative to $B^\pm \to K^\pm \mu^+ \mu^-$.
  - New physics effects could be more pronounced.
- $B^\pm \to \pi^\pm \mu^+ \mu^-$ is a key piece in a complete picture of the flavour structure of these tensions.
- There is an existing binned (in q^2) measurement of $\mathcal{B}(B^\pm \to \pi^\pm \mu^+ \mu^-)$ and $A_{CP}(B^\pm \to \pi^\pm \mu^+ \mu^-)$ (Run 1 of LHCb) [1].

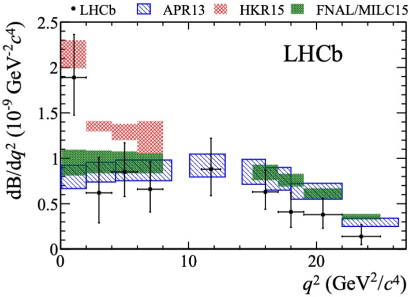

How do we maximise the experimental sensitivity to new physics effects?

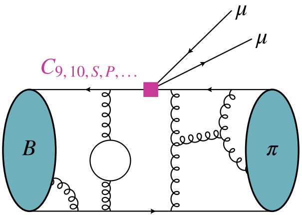

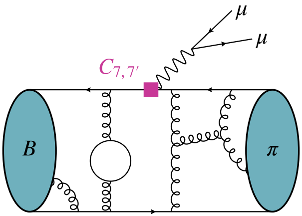

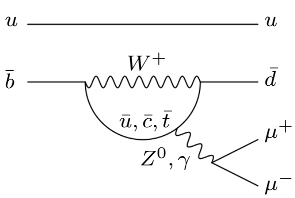

- Recent developments in both theory and experiment now allow for the possibility of unbinned measurements of channels such as $B^\pm \to K^\pm \mu^+ \mu^-$.
- An unbinned approach exploits the full q^2 shape, modelling non-local contributions and any interference.
- The low event yields of this channel motivate incorporating constraints from theory.
- We extract C_9 (+ phase) and C_{10} with an unbinned maximum likelihood fit.

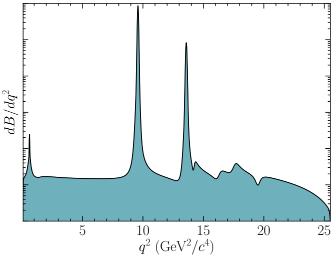

Differences with respect to $B^{\pm} \to K^{\pm}\mu^{+}\mu^{-}$

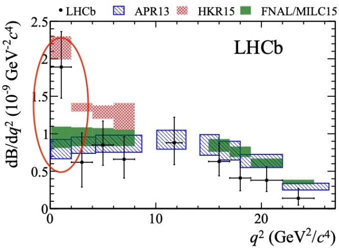

[1]

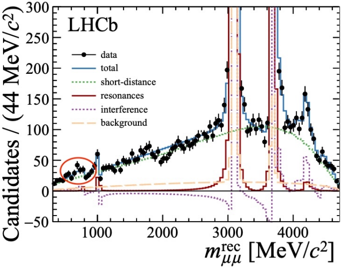

[2]

- $|V_{ts}/V_{td}|^2 \approx 22$ - reduced decay rate across the board.
  - Is this the case for any NP? Is NP minimal flavour violating?
- The ρ and ω resonances are more pronounced (relative to EW penguin mode).
- Relevant contributions from weak annihilation and light quark loops (the light quark continuum).
- Fitting B^{+} and B^{-} events separately is essential due to CP-asymmetries in $B^{\pm} \to \pi^{\pm}\mu^{+}\mu^{-}$ - even in the SM.

Describing the decay rate

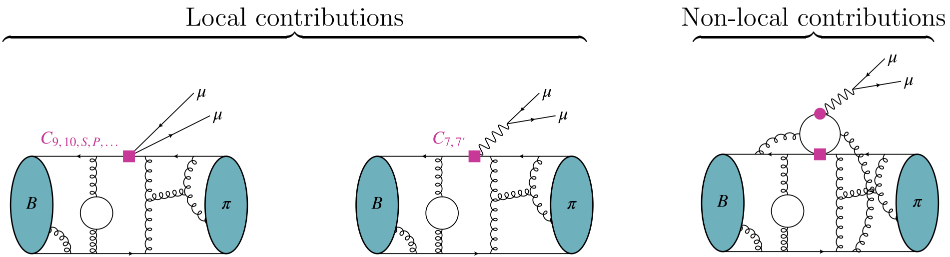

$$\mathcal{L}_{\text{eff}}^{bd\ell\ell} = \frac{4G_F}{\sqrt{2}}\left(\lambda_c\,\mathcal{L}_{\text{eff}}^{(c)} + \lambda_u\,\mathcal{L}_{\text{eff}}^{(u)}\right) + \text{h.c.}, \qquad \text{where} \qquad \lambda_q = V_{qb}V_{qd}^* \qquad \text{and}$$

$$\mathcal{L}_{\text{eff}}^{(p)} = \mathcal{C}_1\mathcal{O}_1^p + \mathcal{C}_2\mathcal{O}_2^p + \sum_{i\in\mathcal{I}}\mathcal{C}_i\mathcal{O}_i \qquad \text{with} \qquad \mathcal{I} = \{3-10, 7'-10', P, P', S, S', T, T5\}$$ [3, 4].

- The matrix elements arising from these effective operators can be classified as either local form factors or non-local form factors.
- Relevant non-local contributions include four-quark operators.
- Relevant local contributions: C_9, C_{10}, C_7

Describing the decay rate

- The kinematics of each $B^{\pm} \to \pi^{\pm}\mu^{+}\mu^{-}$ decay can be fully described with two variables, q^2 and $cos(\theta_\ell)$.
- We integrate over $cos(\theta_\ell)$.

The differential decay rate (over q^2) is then as follows[1] [5]:

$$\frac{d\Gamma(B^{\pm} \to \pi^{\pm}\mu^{+}\mu^{-})}{dq^2} = \frac{G_F^2 \alpha^2 |V_{tb}V_{td}^*|^2}{2^7\pi^5}|k|\left\{\frac{2}{3}|k|^2\beta_+^2|C_{10}f_+(q^2)|^2 + \frac{m_\ell^2(M_B^2 - M_\pi^2)^2}{q^2 M_B^2}|C_{10}f_0(q^2)|^2 + |k|^2\left[1 - \frac{1}{3}\beta_+^2\right]\left|C_9^{\mathrm{eff},B^{\pm}}(q^2)f_+(q^2) + 2C_7\frac{m_b + m_d}{M_B + M_\pi}f_T(q^2)\right|^2\right\},$$

where the non-local contribution ($\Delta C_9^{B^{\pm}}(q^2)$) is baked into $C_9^{eff,B^{\pm}}$,

$$C_9^{\mathrm{eff},B^{\pm}}(q^2) = |C_9|e^{\pm i\delta_{C_9}} + \Delta C_9^{B^{\pm}}(q^2).$$

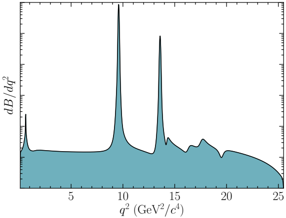

[1] This requires an assumption of no (pseudo-)scalar and (pseudo-)tensor new physics.

Non-local contributions in the $q^2 < 0$ region

- The non-local contributions to $B^\pm \to \pi^\pm \mu^+ \mu^-$ have been computed in the $q^2 < 0$ region by Hambrock et al. as in Ref [6].
- This computation employs operator-product expansion, QCD factorization and light-cone sum rule techniques.
- The full non-local contribution is the sum of the various components:

$$\mathcal{H}^{(p)}\left(q^2\right) = \mathcal{H}^{(p)}_{\text{fact,LO}}\left(q^2\right) + \mathcal{H}^{(p)}_{\text{WA}}\left(q^2\right) + \mathcal{H}^{(p)}_{\text{fact, NLO}}\left(q^2\right) + \mathcal{H}^{(p)}_{\text{soft}}\left(q^2\right) + \mathcal{H}^{(p)}_{\text{soft},O_8}\left(q^2\right) + \mathcal{H}^{(p)}_{\text{nonf,spect}}\left(q^2\right), \quad (p = u, c).$$

- These non-local contributions can then be recast into a shift to the Wilson coefficient C_9 via:

$$\Delta C_9^{B^\pm}(q^2) = -16\pi^2 \frac{(\lambda_u \mathcal{H}^{(u),B^\pm}(q^2) + \lambda_c \mathcal{H}^{(c),B^\pm}(q^2))}{\lambda_t f^+(q^2)}.$$

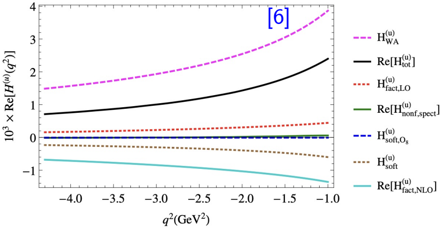

Non-local contributions in the $q^2 < 0$ region

- The non-local contributions to $B^{\pm} \to \pi^{\pm}\mu^{+}\mu^{-}$ have been computed in the $q^2 < 0$ region by Hambrock et al. as in Ref [6].
- This computation employs operator-product expansion, QCD factorization and light-cone sum rule techniques.
- The full non-local contribution is the sum of the various components:

$$\begin{aligned}\mathcal{H}^{(p)}\left(q^2\right) =& \mathcal{H}^{(p)}_{\text{fact,LO}}\left(q^2\right) + \mathcal{H}^{(p)}_{\mathrm{WA}}\left(q^2\right) + \mathcal{H}^{(p)}_{\text{fact, NLO}}\left(q^2\right) \\ &+ \mathcal{H}^{(p)}_{\mathrm{soft}}\left(q^2\right) + \mathcal{H}^{(p)}_{\mathrm{soft},O_8}\left(q^2\right) + \mathcal{H}^{(p)}_{\text{nonf,spect}}\left(q^2\right), \quad (p = u, c).\end{aligned}$$

- From these calculations we have values for $\Delta C_9^{B^{\pm}}$ at various points in negative-q^2.
- We need to build a model for the non-local contributions that we can use to fit the data in the positive q^2 region.

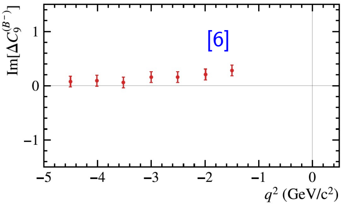

Modelling the non-local contributions - $Y_{light\ quark\ continuum}(q^2)$

To fit $d\Gamma(B^\pm \to \pi^\pm\mu^+\mu^-)/dq^2$ to data we build a model of $\Delta C_9^{B^\pm}(q^2)$,

$$\Delta C_9^{B^\pm}(q^2) = \Delta C_9^{B^\pm}(q_0^2) + Y_{\rho,\omega}^{B^\pm}(q^2) + Y_{LQC}^{B^\pm}(q^2) + Y_{J/\psi,\psi(2S),\ldots}^{B^\pm}(q^2) + Y_{2P,c\bar{c}}^{B^\pm}(q^2),$$

where the subtraction term $\Delta C_9^{B^\pm}(q_0^2)$ is matched to the results of the LCSR+QCD factorisation calculations at the subtraction point q_0^2.

- This contribution is significant in $B^\pm \to \pi^\pm\mu^+\mu^-$, but very small in $B^\pm \to K^\pm\mu^+\mu^-$.
- In $B^\pm \to \pi^\pm\mu^+\mu^-$, both the rare mode ($V_{tb}V_{td}^*$) and these light quark diagrams ($V_{ub}V_{ud}^*$) go as $\sim \lambda^3$.
  - In contrast, in $B^\pm \to K^\pm\mu^+\mu^-$ the rare mode ($V_{tb}V_{ts}^*$) goes as $\sim \lambda^2$.

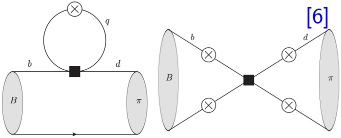

[6]

$Y_{light\ quark\ continuum}(q^2)$

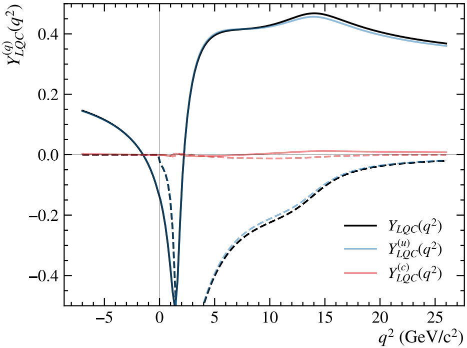

Modelling the non-local contributions - $Y_{c\bar{c}}^{2P}(q^2)$

To fit $d\Gamma(B^{\pm} \to \pi^{\pm}\mu^{+}\mu^{-})/dq^2$ to data we build a model of $\Delta C_9^{B^{\pm}}(q^2)$,

$$\Delta C_9^{B^{\pm}}(q^2) = \Delta C_9^{B^{\pm}}(q_0^2) + Y_{\rho,\omega}^{B^{\pm}}(q^2) + Y_{LQC}^{B^{\pm}}(q^2) + Y_{J/\psi,\psi(2S),\ldots}^{B^{\pm}}(q^2) + Y_{2P,c\bar{c}}^{B^{\pm}}(q^2),$$

where the subtraction term $\Delta C_9^{B^{\pm}}(q_0^2)$ is matched to the results of the LCSR+QCD factorisation calculations at the subtraction point q_0^2.

- We include the combination of the non-resonant continuum of open charm states and the contributions due to further broad vector charmonnia following the recipe of Cornella et al. [7].
- Includes the following rescatterings:

$$B^{\pm} \to \pi^{\pm} M M' \to \pi^{\pm}\mu^{+}\mu^{-},$$

$$\text{where} \quad MM' = \{DD, DD^{*}, D^{*}D^{*}\}.$$

$Y_{c\bar{c}}^{2P}(q^2)$

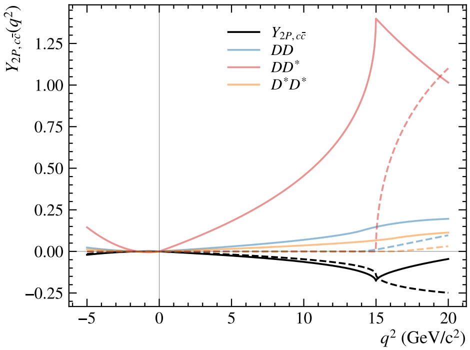

Modelling the non-local contributions - $Y_{c\bar{c}}^{2P}(q^2)$

To fit $d\Gamma(B^{\pm} \to \pi^{\pm}\mu^{+}\mu^{-})/dq^2$ to data we build a model of $\Delta C_9^{B^{\pm}}(q^2)$,

$$\Delta C_9^{B^{\pm}}(q^2) = \Delta C_9^{B^{\pm}}(q_0^2) + Y_{\rho,\omega}^{B^{\pm}}(q^2) + Y_{LQC}^{B^{\pm}}(q^2) + Y_{J/\psi,\psi(2S),\ldots}^{B^{\pm}}(q^2) + Y_{2P,c\bar{c}}^{B^{\pm}}(q^2),$$

where the subtraction term $\Delta C_9^{B^{\pm}}(q_0^2)$ is matched to the results of the LCSR+QCD factorisation calculations at the subtraction point q_0^2.

- To reduce the number of fit parameters, we approximate the sum of DD, D^*D^* and DD^* contributions as a single component with a global magnitude and phase.

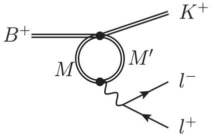

- Exact effect from $B \to DD^* \to \pi\mu\mu$ amplitudes remains remains an open question Ref [8].

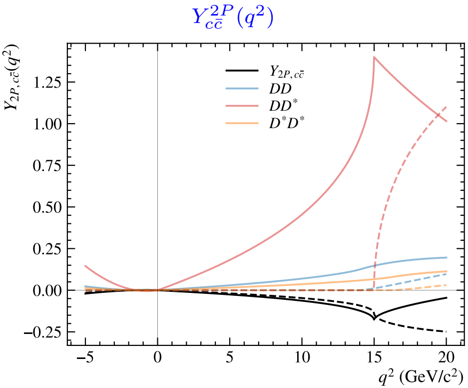

Modelling the non-local contributions - Resonances

To fit $d\Gamma(B^{\pm} \to \pi^{\pm}\mu^{+}\mu^{-})/dq^2$ to data we build a model of $\Delta C_9^{B^{\pm}}(q^2)$,

$$\Delta C_9^{B^{\pm}}(q^2) = \Delta C_9^{B^{\pm}}(q_0^2) + Y_{\rho,\omega}^{B^{\pm}}(q^2) + Y_{LQC}^{B^{\pm}}(q^2) + Y_{J/\psi,\psi(2S),\ldots}^{B^{\pm}}(q^2) + Y_{2P,c\bar{c}}^{B^{\pm}}(q^2),$$

where the subtraction term $\Delta C_9^{B^{\pm}}(q_0^2)$ is matched to the results of the LCSR+QCD factorisation calculations at the subtraction point q_0^2.

- The resonances[1] are described with relativistic Breit–Wigner distributions.
- Each resonance has a unique phase ($\delta_V^{B^{\pm}}$) and a unique magnitude ($\eta_V^{B^{\pm}}$) for both the B^+ and the B^- model.
- We introduce constraints on resonance branching fractions using existing measurements ($BF \propto \eta_V^2$).
- We fix both $\eta_{J/\psi}^{B^{\pm}}$ in the fit - uncertainty included as a systematic.

$|Y_{\rho,\omega}(q^2) + Y_{J/\psi,\psi(2S),\ldots}(q^2)|^2$

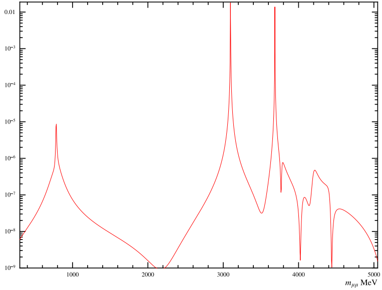

[1] $\rho(770)$, $\omega(782)$, J/ψ, $\psi(2S)$, $\psi(3770)$, $\psi(4040)$, $\psi(4160)$, and the $\psi(4415)$

$B \to \pi$ local form factors

- In the case of $\bar{B} \to \pi$ transitions, there exist only three local $\bar{B} \to \pi$ form factors.

$$\langle \bar{\pi}(k)|\bar{b}\gamma^\mu d|\bar{B}(p)\rangle = \left[(p+k)^\mu - \frac{M_B^2 - M_\pi^2}{q^2} q^\mu\right] f_+(q^2) + \frac{M_B^2 - M_\pi^2}{q^2} q^\mu f_0(q^2),$$

$$\langle \bar{\pi}(k)|\bar{b}\sigma^{\mu\nu} q_\nu d|\bar{B}(p)\rangle = \frac{i}{M_B + M_\pi}\left[q^2(p+k)^\mu - (M_B^2 - M_\pi^2)q^\mu\right] f_T(q^2).$$

- Taken from Leljak et al. [9].
- Take the nominal $K = 4$ LCSR+LQCD option.
  - K is the maximal order of the z-expansion.
- In our fit the form factor parameters are fixed.
- We assess an uncertainty on the Wilson coefficients as a systematic using the covariance matrix provided in Ref [9].

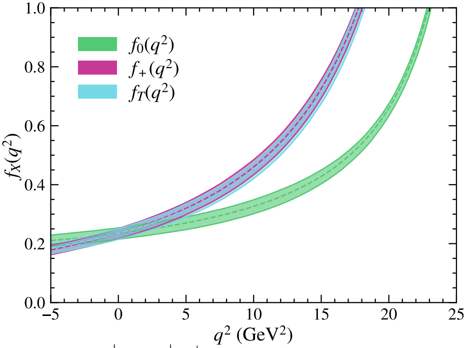

$B^{\pm} \to \pi^{\pm}\mu^{+}\mu^{-}$ decay rate model

- We take the q^2 shape of the efficiency $\varepsilon(q^2)$ from Ref. [2].
- We also take the experimental q^2 resolution used in the LHCb analysis of decays in Ref. [2].
  - Our choice is motivated by the expectation that this resolution is close to if not identical to the LHCb resolution for decays.
- The resolution is folded into the decay rate model using a fast Fourier transform-based convolution,

$$R({q^2}_{\text{reco}}, q^2) \otimes \left(\frac{d\Gamma}{dq^2} \varepsilon(q^2) \right).$$

Below is the signal PDF employed in our toy studies that includes these experimental effects.

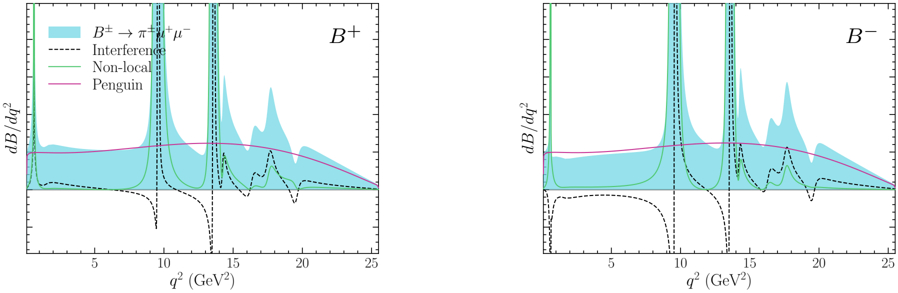

Constraining the non-local contribution

$\mathrm{Re}(\Delta C_9^{B^\pm})$ and $\mathrm{Im}(\Delta C_9^{B^\pm})$ have been computed at various q^2 points in the $q^2 < 0$ region and presented in Ref [6] along with uncertainties.

- We extend the likelihood used in the minimisation of our fits to include a theory constraint term.
- This term minimises the distance between the model of the non-local contribution and the theory reference values.
- This distance is computed at each $q^2 < 0$ point presented in red, and is computed for both the real and imaginary parts of both B^+ and B^-.
- **We do not have access to the correlations between the individual pieces of the $q^2 < 0$ information, so in our fits we make the assumption of no correlations (a conservative choice).**

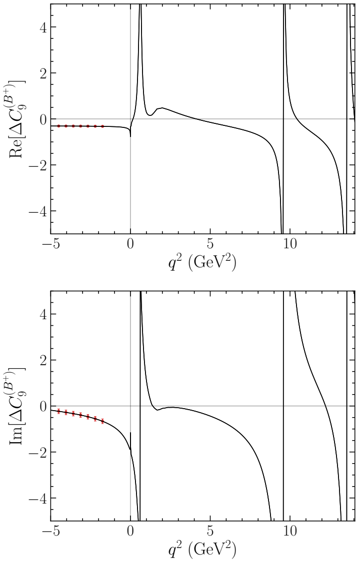

Sensitivity studies

Use toys to study fit stability and to estimate expected precision.

- We run toys at the SM, using values for the non-local parameters as obtained from fits to negative q^2 points.
  - Note that the model obtained is compatible with that of Ref. [6].
- Fit B^+ and B^- simultaneously sharing C_{10}, C_9 and the phase of C_9 (flipping sign under CP).
- Fix the light quark continuum contribution ($Y_{light\ quark\ continuum}(q^2)$).
- Float both the phase and magnitude the $Y^{2P}_{c\bar{c}}(q^2)$ component, sharing the component between B^+ and B^-.

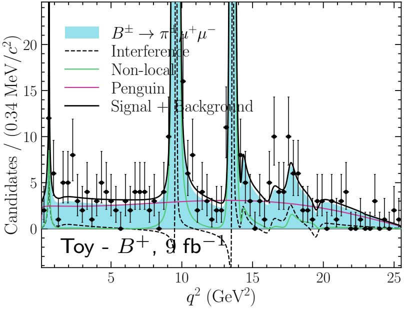

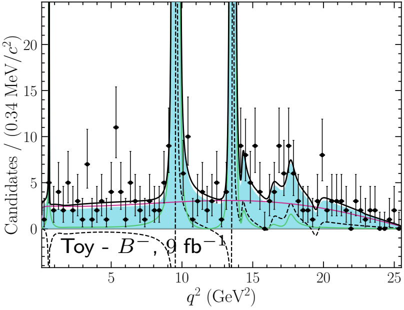

Choosing a q^2 region to fit

- With the expected candidate yields in LHCb Run1+2 it is no surprise that we cannot float the parameters of the open charm resonances.
- We fix these parameters to the $B^+ \to K^+\mu^+\mu^-$ measurements of Ref. [2] scaled by $|V_{cd}/V_{cs}|$ and limit the phase space to $q^2_{\text{reco}} < 14.0625\ \text{GeV}^2$.
  - This is such that contributions from q^2_{TRUE} above the $\psi(3770)$ are negligible even after accounting resolution effects.

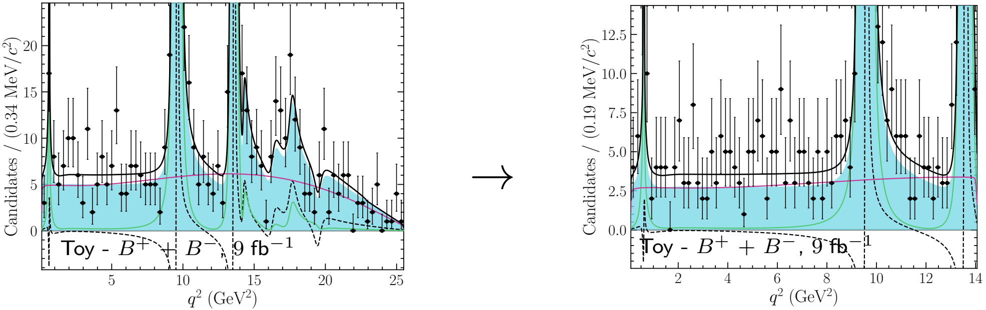

- We find this cut not to be necessary when we study fit stability with a future LHCb data set where we can fit the full q^2 phase space.

Fit stability

- With the LHCb Run 1+2 dataset, there is a significant chance that the best-fit point lies in an unphysical region.
  - Unrealistic without imposing some assumption on NP? $C_9^{\rm NP} = -C_{10}^{\rm NP}$?
- A fraction of fits fail with $C_{10} \approx 0$.
  - There is a discontinuity at $C_{10} = 0$, due to the presence of $|C_{10}|^2$ in the PDF.
- Reparametrising the likelihood in terms of $|C_{10}|^2$ (rather than C_{10}), we find a fraction of fits to pseudo-datasets converge with negative values of $|C_{10}|^2$.
- We label these as failed fits.
- **Fraction of failed fits reduces when employing the $q^2 < 0$ constraint and when increasing event yields.**

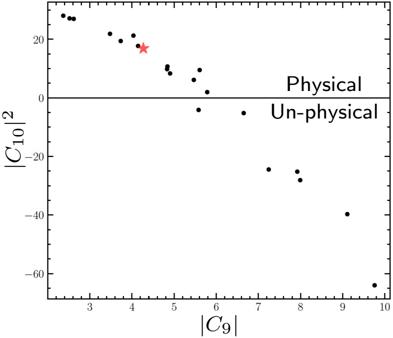

Impact of employing the $q^2 < 0$ constraint

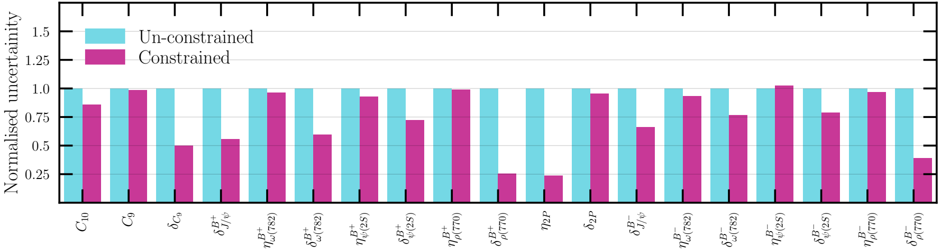

- Run fits to generated pseudo-datasets representative of 45 fb^{-1} of LHCb data ($\times 5$ Run 1+2).
- Fit each dataset both with and without the $q^2 < 0$ constraint.
- Largest improvements are in the phases of the resonances, and the magnitude of the $Y^{2P}_{c\bar{c}}(q^2)$.
- **This increase in sensitivity to non-local parameters translates into better precision on the Wilson coefficients describing the short-distance physics.**

Impact of employing the $q^2 < 0$ constraint

- Intervals from fit results to an ensemble of toys representing $45\ \text{fb}^{-1}$ of LHCb data.

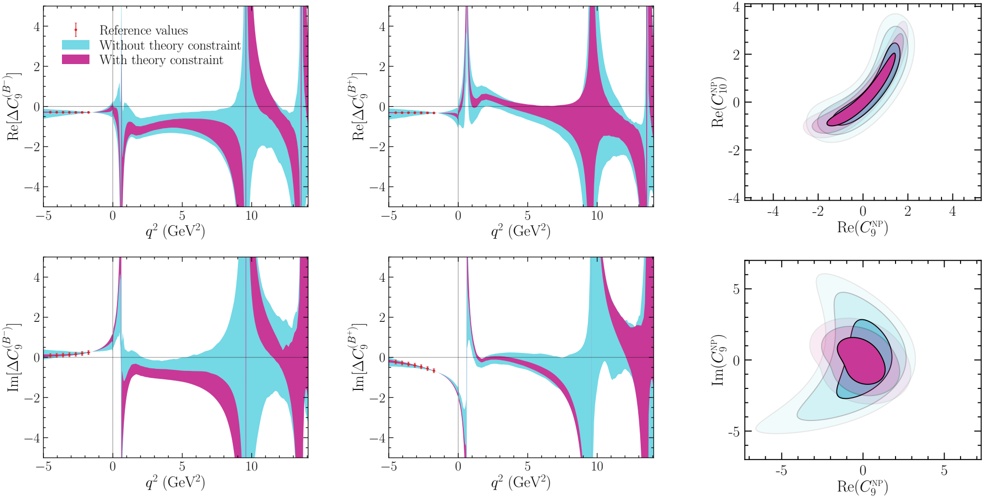

How does the picture change with more data?

- With 300 fb^{-1} the expected $B^{\pm} \to \pi^{\pm}\mu^{+}\mu^{-}$ event yields are similar to those expected of LHCb Run1+2 $B^{\pm} \to K^{\pm}\mu^{+}\mu^{-}$ yields.
- We can then float the open charm resonance parameters.

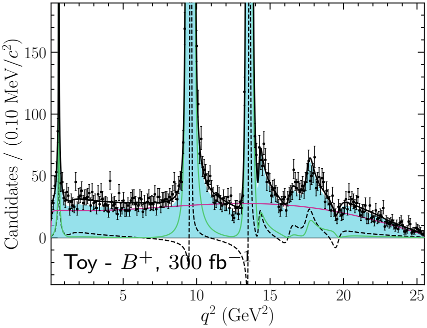

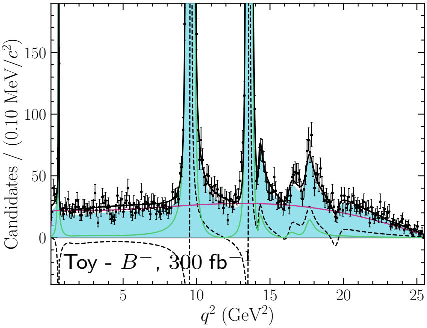

Addressing systematic uncertainties

- Compute the systematic uncertainty accounting for choice to fix the local form factor parameters, $\eta^{B^+}_{J/\psi}$ and $\eta^{B^-}_{J/\psi}$.
- This computation is done separately for the 45 fb^{-1} and 300 fb^{-1} scenarios due to inclusion of the open charm region.
- Fold the systematic into the intervals.

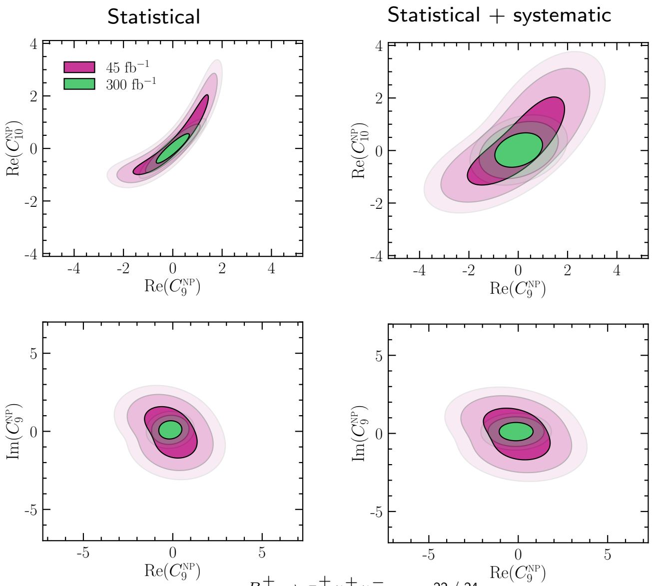

Local form factor uncertainties

- Local form factors uncertainties dominate the systematic uncertainty for all the rare mode parameters: $\mathrm{Re}(C_{10})$, $\mathrm{Re}(C_9)$ and $\mathrm{Im}(C_9)$.
- We stress the importance of addressing form factor uncertainties alongside the coming increase in event yields from future runs of the LHC.
  - Even with Run 4 ($45\ \mathrm{fb}^{-1}$) we are limited by FF uncertainties.
- As an example we show the intervals obtained ($300\ \mathrm{fb}^{-1}$) if we had improved uncertainties (assume 3 times smaller).
  - This improvement would be in line with that achieved for $B \to K^{(*)}$ in Ref. [10].

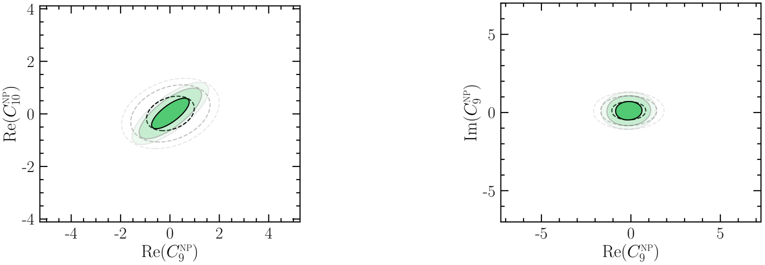

Conclusion - $B^{\pm} \to \pi^{\pm}\mu^{+}\mu^{-}$

- We present an unbinned approach that fully accounts for CP-violation, the largest non-local contributions and all interference effects.
- Employing $q^2 < 0$ information is essential to maximise sensitivity.
- Systematic uncertainties are dominated by knowledge of the local form factors, we emphasise the importance of improving local form factor uncertainties as LHCb takes more data.
- Fitting the current LHCb data set is impractical due to issues of fit stability.
  - We have begun an analysis that will assume $C_9^{\text{NP}} = -C_{10}^{\text{NP}}$
- This work has been submitted to JHEP (2310.06734).

Thanks for listening

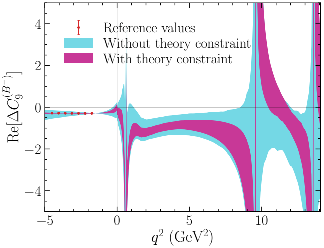

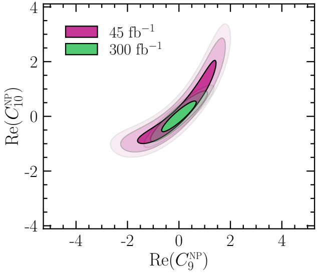

References i

[1] LHCb collaboration, *First measurement of the differential branching fraction and CP asymmetry of the $B^{\pm} \to \pi^{\pm}\mu^{+}\mu^{-}$ decay*, *JHEP* **10** (2015) 034 [1509.00414].

[2] LHCb collaboration, *Measurement of the phase difference between short- and long-distance amplitudes in the $B^{+} \to K^{+}\mu^{+}\mu^{-}$ decay*, *Eur. Phys. J. C* **77** (2017) 161 [1612.06764].

[3] C. Bobeth, M. Misiak and J. Urban, *Photonic penguins at two loops and m_t dependence of $BR[B \to X_s l^{+} l^{-}]$*, *Nucl. Phys. B* **574** (2000) 291 [hep-ph/9910220].

[4] C. Bobeth, A.J. Buras, F. Kruger and J. Urban, *QCD corrections to $\bar{B} \to X_{d,s}\nu\bar{\nu}$, $\bar{B}_{d,s} \to \ell^{+}\ell^{-}$, $K \to \pi\nu\bar{\nu}$ and $K_L \to \mu^{+}\mu^{-}$ in the MSSM*, *Nucl. Phys. B* **630** (2002) 87 [hep-ph/0112305].

[5] A. Ali, A.Y. Parkhomenko and A.V. Rusov, *Precise Calculation of the Dilepton Invariant-Mass Spectrum and the Decay Rate in $B^{\pm} \to \pi^{\pm}\mu^{+}\mu^{-}$ in the SM*, *Phys. Rev. D* **89** (2014) 094021 [1312.2523].

[6] C. Hambrock, A. Khodjamirian and A. Rusov, *Hadronic effects and observables in $B \to \pi\ell^{+}\ell^{-}$ decay at large recoil*, *Phys. Rev. D* **92** (2015) 074020 [1506.07760].

[7] C. Cornella, G. Isidori, M. König, S. Liechti, P. Owen and N. Serra, *Hunting for $B^{+} \to K^{+}\tau^{+}\tau^{-}$ imprints on the $B^{+} \to K^{+}\mu^{+}\mu^{-}$ dimuon spectrum*, *Eur. Phys. J. C* **80** (2020) 1095 [2001.04470].

[8] M. Ciuchini, M. Fedele, E. Franco, A. Paul, L. Silvestrini and M. Valli, *Constraints on lepton universality violation from rare B decays*, *Phys. Rev. D* **107** (2023) 055036 [2212.10516].

[9] D. Leljak, B. Melić and D. van Dyk, *The* $\overline{B} \to \pi$ *form factors from QCD and their impact on* $|V_{ub}|$, *JHEP* **07** (2021) 036 [2102.07233].

[10] N. Gubernari, M. Reboud, D. van Dyk and J. Virto, *Dispersive Analysis of* $B \to K^{(*)}$ *and* $B_s \to \phi$ *Form Factors*, 2305.06301.

BACKUP SLIDES